Article ID: 1006-8775(2004) 01-0087-08

AN OPERATIONAL AUTO-MONITORING FOR THE EL NIÑO EPISODES USING GMS T_{BB}

MA Lan (**马　岚**), JIANG Ji-xi (**江吉喜**), LI Xiao-long (**李小龙**), Wu Xiao Jing (**吴晓京**)

(*National Satellite Meteorological Center, CMA, Beijing* 100081 *China*)

ABSTRACT: By making full use of GMS T_{BB} data, diagnosis and analysis of the formation and development of El Niño **event in 2002 and 2003 were made. It suggests that the first clue of the** El Niño **event appeared in December 2001. The event was formed at the end of 2002 after five phases of development, and came into the phase of flourishing in the winter of 2002. From the analysis the dynamics, it is noted that that the position of the ascending branch of Walker cell was moving from the equatorial west Pacific to the equatorial central Pacific in the phase of formation and development of the** El Niño **event. The process of diagnosis shows that it can provide an important clue for forecasting the genesis and development of the** El Niño **episodes.**

Key words: black-body temperature (T_{BB}); El Niño **episodes**; **Walker circulation**

CLC number: P456.7 **Document code:** A

1 INTRODUCTION

Oceans of the world cover about seventy percent of the earth surface, with larger proportion at the tropics. The tropical oceans not only provide heat energy and vapor, but also change the heat status and therefore make positive effect upon atmospheric circulation. El Niño is a kind of abnormal event taking place within the tropical atmosphere that result from interactions between tropical atmosphere and ocean. The response of tropical atmospheric circulation to the heating of the ocean shows that it has upright latitude circulation corresponding with sea surface temperature (SST) in the tropical atmosphere. Under the normal condition, the sink branch of the circulation is in the cold SST region over the equatorial east Pacific, the ascending branch of the circulation is over the warm SST region at the equatorial west and central Pacific[1]. It is known as the Walker cell.

Many scientists summarized the process of the El Niño event as the ascending branch of Walker cell moving eastward to the region between New Guinea and international dateline in October and November the year before El Niño episodes onset. In this situation, the rainfall decreases over Indonesia, but increases over the nearby region of international dateline. In the prime period of El Niño, large areas of positive SST anomaly cover the equatorial east Pacific, while the west wind over west region of international dateline converges in the ascending branch of Walker cell over the equatorial central Pacific, i.e. convective clouds develop abnormally over the equatorial east and central Pacific, but weaken abnormally over the equatorial west Pacific.

On international research domain of El Niño event, the central and east Pacific region around the equator is separated into four regions. The Nino-4 region is important in the mid-Pacific region. Historical monthly mean anomaly of SST shows that there are abnormal warming phenomena in each part of the ocean during El Niño onset period, only that the value has a little difference. According to an analysis made by Li et al.[7] on basic characteristics of all El Niño

Received date: 2003-05-08; **revised date:** 2004-03-10

Biography: MA Lan (1960 –), female, native from Beijing, senior engineer, undertaking the applied research on satellite remote-sensing information.

episodes beginning from 1951, five out of nine episodes belong to the type of central and upper intensity onset, mainly appearing after the 1980's with higher intensity. So we can study the relationship between the convective cloud region formation and the development of El Niño episodes with the data from the region. The detection scope of GMS is from 70 E to 160 W, which covers the central and west parts of the Pacific on the whole.

The first Geostationary Meteorological Satellite (GMS-1) was launched by Japan on July 14, 1977. The satellites of GMS series have been in operational status since then. The operational satellite at present is GMS-5. There were some modifications based on the problems of the previous satellite from GMS-1 to GMS-5. The GMS-5 that is now operating was launched on March, 1995. One of the important changes of GMS-5 comparing with its four predecessors was that it carried four channels of the Visible and Infrared Spin Scan Radiometer (VISSR) replacing just two channels of VISSR. Besides, in addition to the increase of one more water vapor channel (6.5-7.0μm), the original infrared channel (10.5-12.5μm) was split into two channels (10.5-11.5μm and 11.5-12.5μm).

On the tropical ocean surface, especially near the equatorial region, as the underlying surface is almost homogeneous over the ocean region, convective cloud are of uniform and single nature, yielding almost the same T_{BB} value of the split-window channels.

The GMS T_{BB} data used here are retrieved from the 10.5-12.5μm and 11.5-12.5μm channels, respectively. The retrieval results of the 10.5-12.5μm channel cover the period from 1980 to 1994 and those of the 11.5-12.5μm channel data from 1997 to 2002. For there are some calibration troubles when GMS-4 was replaced by GMS-5, the data from1995 to 1996 was absent.

This paper presents the operational auto-monitoring technique for El Niño episodes developed by the National Satellite Meteorological Center (NSMC). It is able to monitor the whole process of El Niño episodes from initiating, developing to extinction, and provide some important forecasting clues based on the activities of tropical severe convective cloud action as indicated by the black body temperature (T_{BB}) from GMS.

2 METHOD AND DATA

In the detection data of meteorological satellites within the infrared spectrum, the earth is usually used as a blackbody. The radiant rate does not change with the wavelength and the radiance from the earth approaches that from the black body. So the earth is treated as black body. In accordance to Plank's law[8], viz:

$$B(\lambda,T)=\frac{2\pi hc^2}{\lambda^5(e^{hc/\lambda kT}-1)}$$

in which $c=2.9979\times10^8$(m/s) is the speed of light, $h=6.626\times10^{-34}$(J/s) is the Planck constant, $k=1.38\times10^{-23}$(J/K) is the Boltzmann constant, λ is the wave length, and T is called black-body temperature (T_{BB}).

The GMS satellite infrared channels (wavelength from 10.5 to 12.5μm) can be used to detect radiance of the earth surface transmitting from cloud top and areas of no or little cloud . Thereby with the Plunk law radiance could be converted into brightness temperature. According to the research results, the high value region of T_{BB} is cloudless or with few clouds; the low value region is cloudy(for instance $T_{BB}<0$°C. Large-scale atmospheric circulation over the tropics is of direct heat circulation[9]. In these regions, both convection and rainfall are strong, so T_{BB} can be used to indicate the intensity of tropical convective cloud, i.e. the high value of T_{BB} corresponds to the sinking movement of the atmosphere while the low value of T_{BB} corresponds to the ascending movement. The lower the T_{BB} value is, higher the convective cloud development top will be and more vigorous the convective action will be, too.

Based on day-to-day average data of T_{BB} from 1980 to 2000 (except 1995 and 1996)[10],

we calculated the average value and anomaly value on each longitude from January 2001 to December 2002, within the region (5°S – 5°N, 80°E – 160°W)(Fig.1), through quality verification and judgement. We also made longitude-time section plane figures of pentad average and anomaly (Fig.2). In addition, we also calculated monthly anomaly for the region of Nino-4 (5°S – 5°N, 160°E – 160°W) and 5°S – 5°N, 100°E – 160°E from January 1980 to December 2002, and making evolution graph of month by month anomaly (Fig.4). These figures combining with each other become the basic principles of ENSO episodes monitoring.

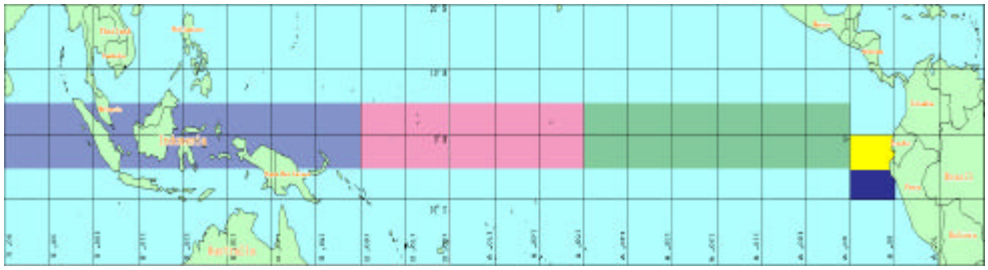

Fig.1 The sketch map of the regions for monitoring El Nino episodes.

3 MONITORING AND ANALYSIS OF EL NIÑO

According to the report from inside and outside of our country about El Niño episodes monitoring, the first El Niño event of this century formed in May 2002 and it is continuing and having middle-level intensity. The whole processes of its formation, development and persistence were monitored with the satellite data and some auspice information of its formation was found.

3.1 *T_{BB} pentad average and anomaly analysis*

Fig.2 is a time-longitude section plane figure. In Fig2a, different levels of grayness represent different value. In both Fig.2a and Fig.2b the region from 80°E to 100°E is in the equatorial east Indian Ocean, the region from 100°E to 160°E is in the equatorial west Pacific, the region from 160°E to 160°W is in Nino-4. It is necessary to demonstrate that the east and west boundary of Nino-4 region is from 160°E to 150°W, but the observation region of GMS is only to 160°W, so the data from these regions had to be used..

The El Niño episode brewing and forming could be divided into five phases.

The first phase: An obvious change on the equatorial east India Ocean (80°E – 100°E) was that the action of convective cloud weakened from December 2001 to January 2002. The weakened change was not seasonal, because Fig.2(b) shows that the region of T_{BB}>15℃ appeared during the period, indicating that convective cloud action over the equatorial east India Ocean anomalously weakened. At the same time, the convective cloud action over the equatorial central Pacific (160°E and nearby) was remarkably reinforced. In the corresponding figure, there was a –25℃ to –35℃ negative anomaly region, showing that there are anomalouis convective cloud action in these regions. We can deduct that the temperatures of these ocean regions ascended. We could call this phase as a reverse process of convective cloud action over the two oceanic regions.

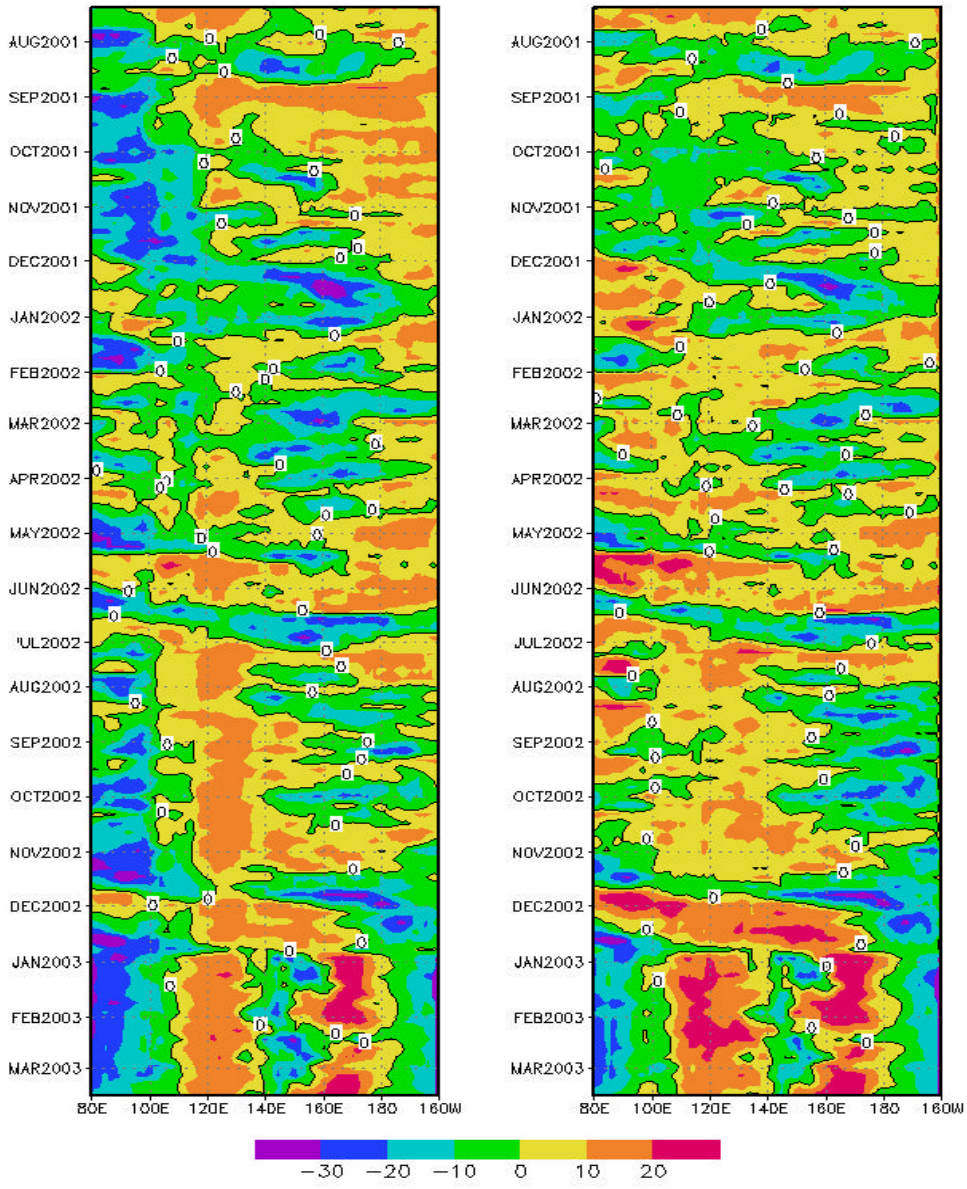

Fig.2 The time-longitude section plane of T_{BB} pentad average(left) and anomaly(right) at the region 5°S – 5°N, 80°E – 160°W from August 2001 to March 2003.

The second phase: The convective cloud region over the equatorial east Indian Ocean and the equatorial central Pacific strenghened and weakened at the same time. It clould be explained in detail that the convective cloud formed over the two oceanic regions in the middle 10 days and the last 10 day of January. T_{BB} value of the convective cloud region was analyzed using the data from the anomaly figure. The result is that the T_{BB} value is from −15℃ to -25℃, lower than that of the same historical period, suggesting that the convection is stronger than that in the history. The convective cloud of the two oceanic regions disappeared in the first ten days of Feburay, but in the middle ten days of February the convective

cloud in two regions emerge at the same time, with the convective cloud over the equatorial east Indian Ocean maintaining for a very short time, only ten days. The convective cloud region over the central part of the Pacific not only had a large scale, but also maintained for a long time, before beginning to spread to the east. Besides, a remarkable phenomenon is that the convective cloud action over the equatorial west Pacific (100°E – 160°E) began weakening. The convective cloud is shown weaker than the perennial on the anomaly figure.

The third phase: It repeated the first phase from the last ten- days in February to the first ten days of March The convective cloud in the equatorial east Indian Ocean weakened while the convective cloud over equatorial central Pacific strengthened. Although the sustained time was short than the first phase, but on the anomaly image, the T_{BB} value over the equatorial central Pacific was – 25°C to – 35°C lower than that in the same historical period. It shows the action of convective cloud over the equatorial east Indian Ocean almost disappeared while the action of convective cloud over the equatorial central Pacific flourished anomalously.

The fourth phase: There was a short-time, intermittent flourishing period of convective cloud action over the two ocean regions from the first ten days to the second ten days in March.

The fifth phase: The action of convective cloud almost had certain reverse changes over the two regions from the beginning of March. Especially after May, the process of reverse changes became very clear with certain vibration. May was determined as the beginning of the El Niño episode by the National Climate Center of CMA and some foreign institutions. From then on, the action of convective cloud over the equatorial central Pacific strenghened, and a – 25°C to –35°C negative anomaly region appeared. These suggested that the increase of sea temperature in the region. The strong convective cloud action began from the equatorial central Pacific.

The action of convective cloud over the equatorial west Pacific disappeared after July, especially during the periods of the first and middle ten days of the month, the beginning ten days of October, and the last ten days of October and December. On the anomaly map (Fig.2b), there appeared some positive anomaly regions with T_{BB} over 15°C. It shows that the region was covered by cloudless sky, ascending atomspheric movement was replaced by descending movement. In these periods, the action of convective cloud over the equatorial central Pacific developed persistently(160°E – 160°W, as shown in Fig.2a), especially there exists a low T_{BB} region of – 30°C to –40°Cduring the first ten-days of September and the first ten-days of December respectively. They are – 35°C to –45°C lower than the normal year (Fig.2b). So there was not only deepen convective actions, but also well developed convective movement, which strengened stably. We can deduce preliminarily that the ascending branch of the Walker cell moved eastward to the central Pacific. This deduction will be analyzed and justified in the atmospheric physics field below.

3.2 *Analysisof atmospheric physics field*

Using the divergence circulation distribution map of 200 hPa and 850 hPa published by the National Climate Center[11] (Fig.3), the location changes of the ascending branch of the Walker cell was discussed. Before the onset of the El Niño episode, the strongest divergence wind zone on the earth is the region between the New Guinea island and dateline, with which three east-west circulation cells are correlated: region of Saudi Arabia-Mediterranean, the southwest Indian Ocean and the east Pacific convergence zone which is a high-level branch of the Walker cell. These are identical with research results from others[2-6] [12]. The figure of monthly mean wind speed and convergence wind at 850 hPa distinctly shows that the convergence zone is to the north of New Guinea island and the nearby area, the wind speed of the convergent center is more than 10m/s, the point is the location of the ascending branch of Walker cell.

After the onset of the El Niño episode, the strongest convergent wind zone is over Micronesia, its location is 20 degrees eastward by longitude as compared with the normal years. The three east-west circulation correlated with the convergent

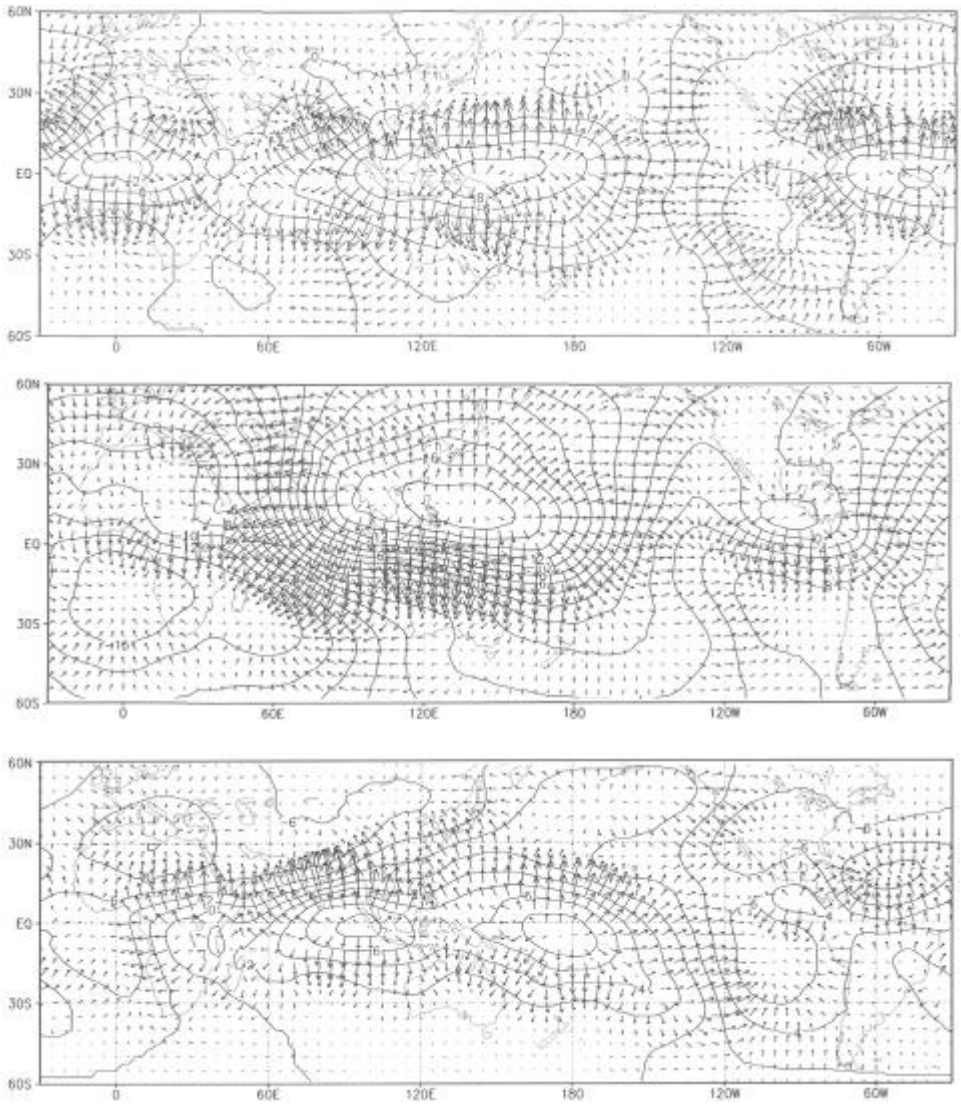

Fig.3 The trend of monthly mean velocity ($10^6 m^2/s$) and divergent wind (m/s) at 200hPa in (a) April, (b) August, and (c) December, 2002.

center are in the north of Africa, southwest of Atlantic and southeast of Pacific. The figure of the same regions of monthly mean wind speed at 850hPa and divergent wind zone are also over the Micronesia, the wind speed at the divergent center is more than 12m/s. In December, with the El Niño blooming (Fig.3c), the strongest divergent wind zone appears near the dateline, and in the corresponding figure (omitted) of monthly mean wind speed and the convergent wind at 850hPa, there is a convergent center with the wind speed more than 10m/s near the dataline.

Therefore, it was diagnosed that the location of the ascending branch of the Walker cell moved from the equatorial west Pacific (near 140°E) to the equatorial central Pacific (near 180°E), these are identical with the result from the analysis

of the action of convective cloud in the T_{BB} pentad average and the anomaly figure. Thus it can be seen that the T_{BB} pentad average and the anomaly time-longitude map(figure 2) can be used not only to monitor the process of tropical convective cloud evolvement, but also to monitor the intensity and movement of the ascending branch of Walker cell.

3.3 *Analysis of the evolution of T_{BB} monthly anomaly difference*

It has been shown by foregoing analysis that there exists a great contrast between the convective cloud over the equatorial central Pacific and that over the equatorial west Pacific after onset of the El Niño episode. The monthly anomaly from the region of Nino-4 (5°S – 5°N, 160°E – 160°W) and the region of the west tropical Pacific (5°S – 5°N, 100°E – 160°E) (Fig.1)was chosen by Jiang[13] to show the difference of the intensity of abnormal convective cloud over these two ocean regions. When the difference is negative, it indicates that the action of convective cloud is more flourish than that in the normal years, and the convective action over the equatorial west Pacific is weaker than that in the normal years. The convective actions over the two oceanic regions are contrary when the difference is positive. Therefore, in addition that the convective action over the oceanic region is remarkably stronger than that on the normal years, it also indicates that the SST is abnormally high. It is contrary when T_{BB} is positive.

Fig.4 is a graph of T_{BB} monthly anomaly in the region 5°S – 5°N and Nino-4 and 100°E – 160°E from January 1980 to February 2002.. It has a first-rate correspondence in the past two decades to the El Niño and La Niña episodes monitored. There appeard La Niña event (autumn 1998 to autumn 2000) after the strongest El Niño event in last century(1997 to 1998). The T_{BB} monthly anomaly value has a peak value of 15°C at the end of 2000/2001, but the peak value decreases rapidly after spring. The general trend of the change of T_{BB} monthly anomaly values decreased in several months of the year. In autumn, the anomaly value is -3°C, it indicates that the convective cloud action over the two regions has completely got rid of the influence of La Niña episodes, and a new El Niño episode will emerge. The first phase of the El Niño event happen in Dec.2001, mentioned above was a period of convective cloud action strengthened abnormally, the low value of the difference of T_{BB} monthly anomaly value is about -6°C. The curve of the difference of T_{BB} monthly anomaly value

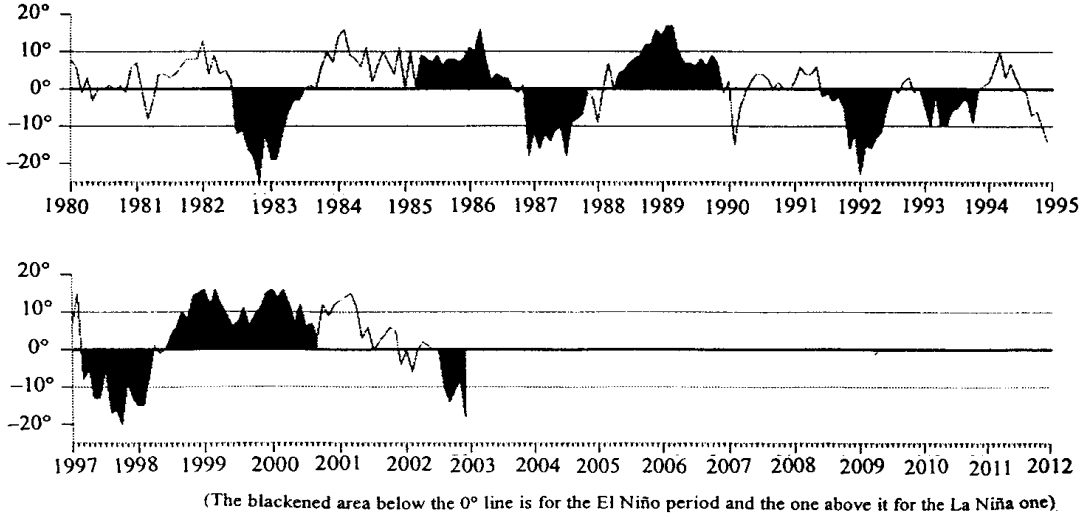

Fig. 4 The curve evolution with time of T_{BB} monthly anomaly difference in the region of Niño-4 and the region of 100°E – 160°E from January 1980 to December 2002.

appears surge, but the general trend is the increasing extent is decreasing. The T_{BB} monthly anomaly difference is always below 0℃ after May 2002, especially there appeared a value of -18℃ that approached the lowest value in El Niño periods of last century. According to the comprehensive view of the change of T_{BB} monthly anomaly difference in autumn of 2000/2002, we find T_{BB} monthly anomaly difference changed to a negative value after experiencing the strongest La Niña event in last century. There are some turbulences, but the peak value decreased gradually. The peak maintaining period shortened gradually. The El Niño event happened after brewing over one year.

4 SUMMARY

a. The original clue of El Niño event appears in Dec.2001, brewing and forming in spring 2002, running to blooming period in winter 2002.

b. In forming and developing the period of the El Niño event, the ascending branch position of the Walker cell moved from the equatorial west Pacific to the equatorial central Pacific.

c. The T_{BB} pentad average and anomaly time-longitude section map can be used to monitor tropical convective cloud evolvement, it also can be used to monitor the intensity and movement of the ascending branch of the Walker cell.

d. The graph of T_{BB} monthly anomaly difference evolution can reflect the whole process of El Niño event formation and development, and can provide important clue to the forecasts for the formation of El Niño episodes. It is an important means in monitoring and seeking the ENSO forecasting clue by utilizing satellite remote sensing data, since we do not clear enough about the forming mechanism of ENSO event.

REFERENCES:

[1] Bjerknes J., A possible response of the atmospheric Hadley circulation to equatorial anomalies of ocean temperature [J]. *Tellus*, 1966,18: 820-829.
[2] Philander S.G.H, El Niño Southern Oscillation phenomena [J]. *Nature*, 1983, 302: 296-301.
[3] CHEN Lie-ting. Effect of SST anomalies in the equatorial eastern Pacific on tropical general circulation and precipitation during the raining season in China [J]. *Chinese Journal of Atmospheric Sciences*, 1977, **1**: 1-12.
[4] LI Chong-yin. On the effect of El Niño episodes on the west Pacific typhoons [J]. *Acta Meteorologica Sinica*, 1987, **45**: 229-236.
[5] ZHANG Ren-he. Tropical Oceans and East Asian Monsoons [A]. Retrospective Reviews and Outlooks for the Atmospheric Sciences in the early 21st Century [M]. Beijing: Meteorological Press, 2000. 115-118.
[6] YU Zhi-hao, JIANG Quan-rong. El Niño, Anti- El Niño and Southern Oscillations [M]. Nanjing: Nanjing University Press, 1994. 68-82.
[7] LI Xiao-yan, ZHAI Pan-pao. ENSO episodes Indexes and studies on indexes [J]. *Scientia Meteorologica Sinica*, 2000, **58**(1): 102-109.
[8] DONG Chao-hua et al. Manual for Interpretation of Meteorological Satellite Products [M]. Beijing: Meteorological Press, 1999. 187-198.
[9] CHAO Ji-ping. Dynamics of El Niño and Southern Oscillations [M]. Beijing: Meteorological Press, 1993. 1-22.
[10] JIANG Ji-xi, FAN Mei-zhu. T_{BB} Atlas and its application [M]. Beijing: Meteorological Press, 2001. 73-132.
[11] National Climate Center. Bulletin of Monthly Climate monitoring [R]. Beijing: Meteorological Press, 2002. 1-12.
[12] DING Yi-hui. Advanced Synoptics [M]. Beijing: Meteorological Press, 1991. 266-277.
[13] JIANG Ji-xi, FAN Mei-zhu. On the Methods of ENSO Monitoring by Meteorological Satellites [A]. On the Monitoring and Prediction of ENSO [M]. Beijing: Meteorological Press, 2000. 18-22.